

# 1

## Self-Assembly of Molecular Metal Oxide Nanoclusters

Laia Vilà-Nadal and Leroy Cronin

University of Glasgow, WestCHEM, School of Chemistry, University Avenue,  
Glasgow G12 8QQ, UK

### 1.1

#### Introduction to Self-Assembly

“[ . . . ] Verily at the first Chaos came to be, but next wide-bosomed Earth, the ever-sure foundations of all [ . . . ].” This sentence is extracted from Hesiod’s Theogony composed around 700 BC, describing the origins and genealogies of the Greek gods [1]. About 300 years later, Democritus formulated atomistic theory and imagined all matter in the universe evolving from its atomistic components to form everything from the Earth to the stars [2]. In exploring this assembly and organization, the ancient questions have barely changed: how an ordered structure such as a natural beehive emerged? Or how to explain the geometrical beauty and the symmetry of a seashell? Complex organized patterns appear to be a feature of living and technologically produced systems.

Descartes published in 1644 the Principles of Philosophy in which he envisioned an ordered universe coming out of chaos obeying nature’s laws through the organization of small objects into larger assemblage; it appears that Descartes himself was envisaging questions that are also relevant to nanoscience [3]. Indeed, the emergence of order from disorder has captivated the imagination of curious individuals for millennia. In our quest to understand, and perhaps control nature, we realized that breaking down and partitioning problems into their smallest components is useful to understand the whole picture, but complex dynamics and stochastic processes are prevalent at these scales.

A classic analogy to explain self-assembly is the following question: put the different parts of a car in a big box, and shake the whole, will you get a car? [4]. If that was even possible, the consequences would be mind-blowing, and have been often explored in fiction literature and films. Self-assembly is not a human creation, it is a spontaneous process and is well studied at smaller scale from atoms and molecules up to the millimeter scale and beyond [5]. The process by which an organized structure spontaneously forms from individual components,

as a result of specific, local interactions among its components, is one of the most widely used definitions of self-assembly [6]. More importantly, at the primal level, the spontaneous organization of complex objects does not appear possible without an energy-consuming machinery, cf. the ribosome.

The concept of self-assembly emerged in the early 80s in organic chemistry. Self-assembly and self-organization are often used interchangeably but they refer to two very different processes, and hence have different meanings [7]. In order to clarify their meanings, we must introduce the concept of equilibrium. A chemical reaction has reached equilibrium when the concentrations of both reactants and products do not change over time. Chemical reactions in which the reactants convert to products and where the products *cannot* convert back to the reactants are an example of an irreversible process that leads to entropy production [8]. Therefore, a self-assembly reaction leading towards an equilibrium state, in thermodynamic terms, is due to the minimization of free energy in a closed system. Whereas, self-organization occurs far from equilibrium in an open system, since it requires an external energy source. For instance, the Belousov–Zhabotinsky (BZ) reaction, is a classic example of a nonequilibrium, dissipative reaction [9]. Nonequilibrium and dissipative systems have fascinated scientists for decades. Ilya Prigogine was awarded the 1977 Nobel Prize in Chemistry for his contribution to the field [10]. In essence, he discovered that by importing and dissipating energy into a chemical system, the rule of maximization of entropy, imposed by the second law of thermodynamics, was reversed. Simply put, it takes energy to create improbable configurations from disordered ones [11].

Beyond this, we all agree that there are chemical processes which, at equilibrium, do not dissipate energy, and others which are dissipative and far from equilibrium. It has been a challenging mission for the scientific community to establish “what self-assembly is” since the terminology and practice is multidisciplinary, crossing multiple length scales and spanning a range of forces and fields as diverse as cosmology and biology – length scales from nanoscopic to macroscopic and forces from “weak” to “strong” [12]. Whitesides and Grzybowski have defined two types of self-assembly: (a) the static self-assembly resulting in an equilibrium state and energy minimization and (b) the dynamical self-assembly with energy dissipation [5]. A few examples of each type, see also Figure 1.1, are as follows. Static self-assembly: molecular crystals [13], lipid bilayers [14], and polymers [15]. Dynamic self-assembly: oscillating reactions [16] and reaction diffusion reactions [17].

Self-assembly in molecular systems can be determined by a number of characteristics such as the components (building blocks), interactions (balance between attractive and repulsive forces), reversibility (or adjustability), its environment (promotes the motion of its components), and finally mass transport and agitation (for instance, thermal motion to assure molecular mobility) [18]. Whether self-assembling molecular building blocks can form into well-organized structures depends on the ability to control their size, shape, and surface properties. Therefore, one of the main goals of

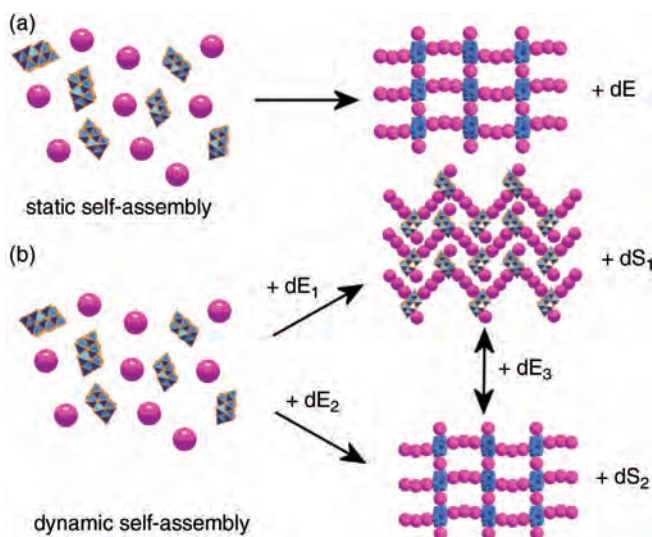


**Figure 1.1** Graphical representation of static self-assembly (a) in which self-organization proceeds to an energetic minimum after an exothermic process releasing energy  $dE$ ; (b) describes a situation out of equilibrium,

dynamic self-assembly that requires a constant flow of energy,  $dE_1$ ,  $dE_2$ , and  $dE_3$ , into the system to be sustainable, generating entropy  $dS_1$  and  $dS_2$ .

self-assembly is being able synthesize building blocks with specified dimensions and forms, and chemically control their surface properties (e.g., charge, hydrophobicity, hydrophilicity, functionality) [19].

Self-assembly also has profound implications in life and origin of life research. One can imagine life as a dynamic self-organized system moving toward, but never reaching, equilibrium; since things at equilibrium are dead as they are not able to process information or self-organize. For example, the organelles of a cell can also be described as a collection of independent parts (or building blocks), each of them designed to perform a specific task. Hence, in our postindustrial society, the assembly line has long been considered one of the greatest innovations of the twentieth century. We can now envisage the power of directed self-assembly at small scales [20].

## 1.2 Molecular Metal Oxides: Polyoxometalates

Metal–oxygen anionic clusters of early transition metals (V, Nb, Ta, Mo, W) in their highest oxidation states constitute a family of compounds known as polyoxometalates (POMs) [21]. One of the founders of modern chemistry Berzelius, in 1826, described the formation of yellow compounds when phosphate and arsenate salts were mixed with molybdic acid [22]. It was not until 1934, when

Keggin carried out the first detailed crystallographic characterization of a POM salt [23]. POMs are still of great interest and are studied by many groups around the world. This is not surprising since POMs are structurally diverse, and their interesting properties have been exploited in multiple scientific fields, for example, catalysis, medicine, and materials science [24–26]. A seminal work in the classification and study of oxoanions and their salts was presented in the 1983 book by Pope [27]. Thanks to the recent technical advances in spectroscopic methods (IR, resonance Raman, visible/near-IR) as well as single-crystal X-ray structure analysis and electrospray ionization mass spectroscopy (ESI-MS) the number of characterized structures of POMs has increased enormously [28]. Understanding their mechanisms of assembly and the development of new applications has required a great effort for several research groups [29,30]. In addition, exploring the organizational aspects of polyoxometalate structures from small fragments to large species has allowed the synthesis of gigantic molybdenum structures [31]. In fact, the category of metal oxide clusters or POMs includes an unprecedented number of anionic multinuclear species that display a large number of structures, compositions, and sizes ranging from 1 to 5.6 nm, see Figure 1.2 [32]. With only six metal units, the smallest cluster is the so-called Lindqvist anion  $[M_6O_{19}]^{n-}$  (in which M = Mo, W, etc.) [33]. The other two iconic structures are known as Keggin (12 metal centered) and Wells–Dawson (18 metal centered) clusters, both members of the heteropolyanions (HPAs) family: metal oxide clusters that encapsulate heteroanions, such as  $[SO_4]^{2-}$ ,  $[PO_4]^{3-}$ , and so on [34]. Another example of a HPA is the Preyssler anion – this is a cluster with 30 W atoms surrounding a large internal cavity [35]. Finally, perhaps some of the most remarkable molecular structures known are those based upon polyoxomolybdates. For instance, the inorganic fullerene  $\{Mo_{132}\}$  belongs to the family of the Keplerate [36] clusters reported by Müller and coworkers. Molybdenum oxide-based fragments, known as Mo-blue or Mo-brown, are reduced Mo-based POMs. Mo-based clusters have a rich structural flexibility under reducing conditions as shown by the isolation of the largest nonbiologically derived molecule to date, a lemon shaped cluster containing 368 molybdenum atoms ( $\{Mo_{368}\}$ , the “Blue Lemon”) [32].

Polyoxometalates can be classified according to their structural characteristics. They are mainly divided into the following three categories:

- 1) *Heteropolyanions (HPAs)* are tungsten, molybdenum, or vanadium metal oxide clusters that encapsulate heteroanions such as  $[SO_4]^{2-}$ ,  $[PO_4]^{3-}$ ,  $[AsO_4]^{3-}$ , and  $[SiO_4]^{4-}$ . The incorporation of a heteroanion in the compound offers a great degree of structural stability in the cluster. For this reason, these are the most explored subset of POM clusters, mostly exploiting their catalytic properties. As stated earlier, the Keggin  $[XM_{12}O_{40}]^{n-}$  and the Wells–Dawson  $[X_2M_{18}O_{62}]^{n-}$  anions (where M = W or Mo; X is a tetrahedral template) are two of the most easily identified structures within the POM family, see Figure 1.2. Tungsten-based structures are the most robust, hence we have exploited their rigidity to develop lacunary derivatives, that is,

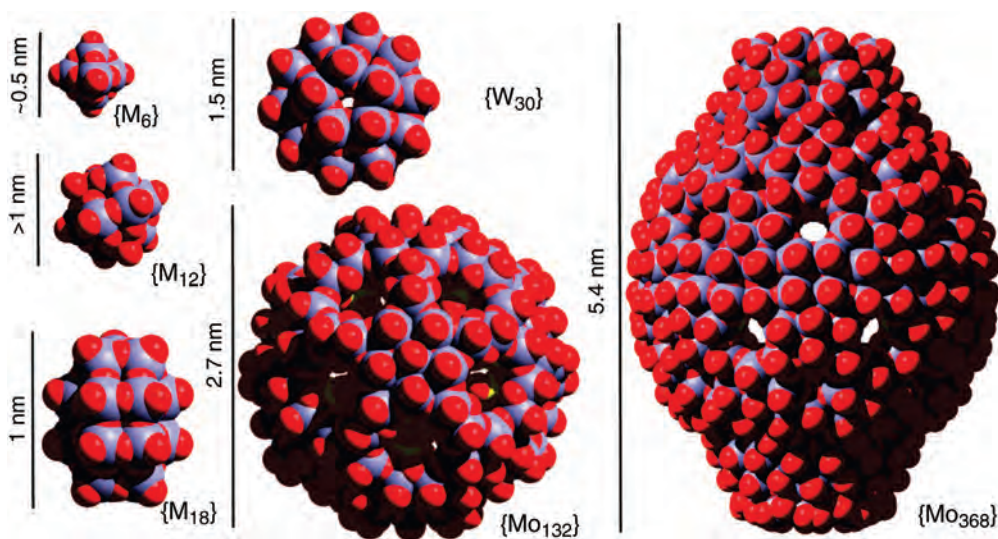


**Figure 1.2** Structures of some POM clusters (space filling models M: blue, O: red, S: yellow). The  $\{M_6\}$  Lindqvist anion  $[M_6O_{19}]^{n-}$  formed by a compact arrangement of six edge-shared  $MO_6$  octahedra. The  $\{M_{12}\}$  Keggin structure  $[(XO_4)M_{12}O_{36}]^{n-}$  composed of four  $M_3O_{13}$  groups of three edge-shared  $MO_6$  octahedra that are linked sharing corners to each other and to the central  $XO_4$  tetrahedron. The  $\{M_{18}\}$  Wells–Dawson structure  $[(XO_4)_2M_{18}O_{54}]^{n-}$  can be seen as two fused Keggin fragments. The  $\{W_{30}\}$  Preyssler anion  $[X^{n+}P_5W_{30}O_{110}]^{(15-n)-}$

with an internal cavity that can be occupied by different cations (Na, Mn, Eu). The Keplerate-type structure  $\{Mo_{132}\}$ , resulting in “spherical disposition” of pentagonal  $\{(Mo)Mo_5\}$  building blocks. The largest cluster to date is the lemon shaped  $\{Mo_{368}\}$  containing 368 metal (1880 nonhydrogen) atoms formed by the linking of 64  $\{Mo_1\}$ , 32  $\{Mo_2\}$ , and 40  $\{Mo(Mo_5)\}$ -type units. The structures of the clusters are compared (to scale) to illustrate the wide range of sizes that POMs can achieve.

- Keggin and Dawson anions with vacancies (most commonly with one, two, or three vacancies) that can be linked using electrophiles to larger aggregates in a predictable manner. The development of lacunary polyoxometalates based upon Keggin  $\{M_{12-n}\}$  and Dawson  $\{M_{18-n}\}$  is a large research area [37].
- 2) *Isopolyanions (IPAs)* are also composed of a metal oxide framework, but in this case without the heteroatom/heteroanion that makes them less stable. However, they are often used as building blocks to construct larger structures, together with their physical properties and high charges and strongly basic oxygen surfaces [38].
  - 3) *Mo-blue and Mo-brown-reduced nanosized POM clusters* were historically described by Scheele in 1783. Their composition was unknown until Müller *et al.* reported the synthesis and structural characterization in 1995 of a very high-nuclearity cluster  $\{Mo_{154}\}$ , which exhibits ring topology, that crystallized from a solution of molybdenum blue [39]. Learning to control the experimental variables of these systems led to the discovery and proper characterization of the first member of the Mo-brown species that exhibited a

porous spherical topology  $\{\text{Mo}_{132}\}$  [40]. This cluster can be formulated as  $[\text{Mo}_2\text{VO}_4(\text{CH}_3\text{OO})]_{30}(\text{Mo})\text{Mo}_5\text{O}_{21}(\text{H}_2\text{O})]_{12}]^{42-}$  and is able to encapsulate over 100 water molecules inside its quasispherical polyoxomolybdate nanocapsule cluster, forming a water nanodrop [36]. The structuring of the water inside the  $\{\text{Mo}_{132}\}$  nanocapsule resembles that of the  $\text{C}_{60}$  fullerene.

### 1.3

#### Mechanisms of Cluster Formation

As we have described, POMs are a diverse set of metal oxide compounds with nucleation number ranging from 6 to 368. The most common synthetic method is a “one-pot” synthesis, but this term only describes the final product of the reaction and the complicated network of interactive chemical processes present in the synthesis is obviated. In fact, this “one-pot” approach is misleading since it seems to indicate that POM systems are directed by simple rules, instead of being the result of self-assembly processes [37]. Synthetic routes to the most common structures are well known, mostly involving an acidification of alkaline aqueous solutions of simple oxoanions, controlling the pH and temperature. After the experience gained by unveiling new structures and optimizing their synthetic methods, it became apparent that POMs are the result of complex networks of chemical reactions governed by several variables. These self-assembly reaction networks allow to establish several equilibria that create a pool of available building blocks to assemble into more complex architectures, controlled by a long list of experimental variables such as: (1) concentration/type of metal oxide anion [38], (2) pH, (3) ionic strength, (4) heteroatom type/concentration, (5) presence of additional ligands, (6) reducing environment, (7) temperature and pressure of reaction (e.g., microwave, hydrothermal, refluxing), (8) counterion and metal-ion effect, and (9) processing methodology (one-pot, continuous flow conditions, 3D printing of reaction ware) [39–42]. New clusters are discovered, and up to some extent even “designed” by controlling the already listed experimental variables. Synthetic experience and careful variable control also helped to generate a vast library of building blocks, and to attempt the design of new POM-based materials.

Despite this synthetic knowledge, few studies have been dedicated to analyze the formation mechanisms of POMs. In fact, the processes of aggregation involved in the formation of these molecules are still poorly understood. Compared with other widely studied characteristics of POMs, such as electronic structure, redox behavior, and magnetic and nonlinear optical properties, the assembly mechanism of POMs still represents a challenge. Recently, the groups of Cronin and Poblet described the nucleation mechanisms of POMs with low nuclearities, by combining theoretical calculations and data from ESI-MS [43]. Standard density functional theory (DFT) calculations combined with molecular dynamics (MD) simulations demonstrate that once the dinuclear species are formed, consecutive steps of protonation and water condensation followed by

aggregation take place. In these studies, we proposed two possible mechanisms involving successive protonation and water condensation steps, both thermodynamically favorable and with effectively no barrier at room temperature.

These results agree with the fragments observed in ESI-MS experiments for Lindqvist anions. These “soft-ionization” approaches are unique since they allow for well-defined resolution of multiple closely related species (in contrast to other common spectroscopic techniques such as UV-vis or IR) and can provide clear, well-resolved “snapshots” of a given system on a time scale down to within tens of seconds, if necessary. In this initial study, we concluded that the Lindqvist  $[M_6O_{19}]^{n-}$  ( $M = Mo, W$ ) anion formed in six consecutive steps that incorporate one metal unit at a time, and globally is an exothermic process [43]. We have also identified a common planar  $[M_3O_{10}]^{2-}$  motif in the most stable tetra- and pentanuclear intermediate clusters that gives a greater stability to these intermediate clusters, see Figure 1.3. A detailed study by Lang *et al.* expanded the understanding of the self-assembly mechanism for the  $[W_6O_{19}]^{2-}$  identifying relative Gibbs free energies and transition states (at 298 K and 1 atm) for the formation process of all the intermediates [44].

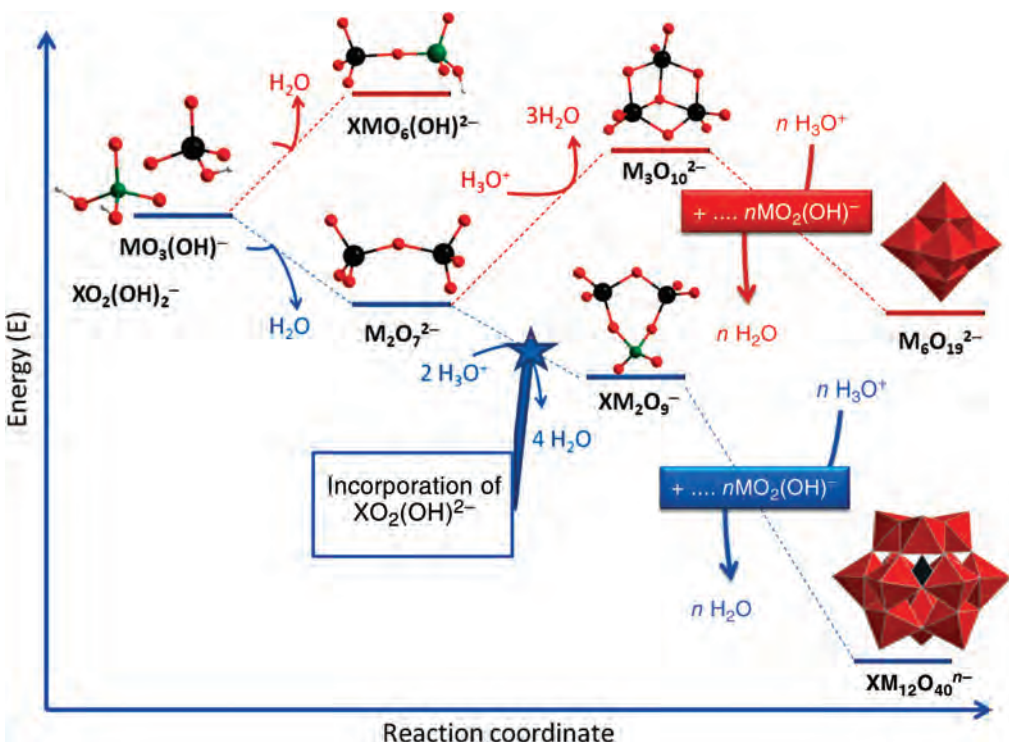


**Figure 1.3** Schematic representation of the initial steps, dimer and trimer, of the formation mechanisms for the Lindqvist  $[M_6O_{19}]^{2-}$  ( $M = W$  and  $Mo$ ) and Keggin  $[XM_{12}O_{40}]^{3-}$  ( $M = W$ ,  $Mo$  and  $X = P$  and  $As$ ) anions.

We have also investigated the first nucleation steps, dimer, trimer, and tetramer, in the formation of the Keggin-type anion. Stoichiometrically obtaining the Keggin anion  $[XM_{12}O_{40}]^{n-}$  requires up to 10 protonations and 12 water condensations. As we have described for the Lindqvist anion, we postulate that once the dinuclear species have been formed, including the isodimer  $[M_2O_6(OH)_2]^{2-}$  that also appears in the first formation step of the Lindqvist anion or the heterodimer  $[MXO_5(OH)_3]^{2-}$ , successive steps of protonation and water condensation with subsequent aggregation occurs to justify the clusters observed in the ESI-MS experiments. We propose that the heteroanion,  $[PO_2(OH)_2]^-$  or  $[AsO_2(OH)_2]^-$ , is not incorporated into the polyanion in the first step of the nucleation, that is, forming a heterodimer, but in a later step [45]. Once the heterotrimer is formed, the heteroanion acts as a template for the formation of the Keggin anion. In both studies, Lindqvist and Keggin anions, we did not find any significant differences between tungstates and molybdates, see Figure 1.3. As a complementary work to our report, Lang *et al.* provided the whole thermodynamic analysis of the consecutive steps for the formation of  $[PW_{12}O_{40}]^{3-}$  and the analysis of intermediate anions [46].

#### 1.4 Isomerism in Polyoxometalates

Another interesting aspect of metal oxo clusters is that despite their structural robustness polyoxometalate structures present rotational isomerism. In fact, the POM clusters can be seen as a sort of “inorganic Rubik’s Cube,” see Figure 1.4. It has been known since two isomers of the Keggin silicomolybdic acid were described in the early 50s by Strickland [47]. Isomerism in POMs has been largely studied and their properties deeply analyzed experimentally and computationally, although some basic points are still not completely clear. The main interest in isomerism is related to the possibility of tuning some properties with

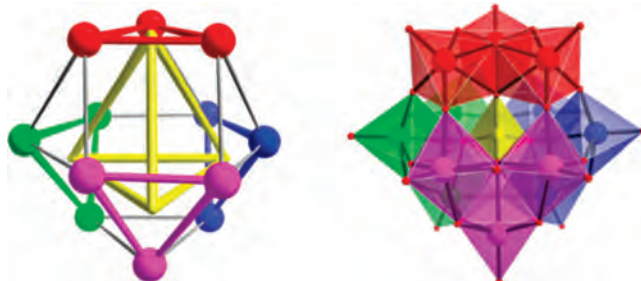


**Figure 1.4** Rationalization of the 12 metal-centered Keggin heteropolyoxoanion structure,  $[\alpha\text{-}XM_{12}O_{40}]^{n-}$ . The anion is composed of four independent  $[M_3O_{13}]$  triads (red, green, magenta, blue) interconnected by threefold

nodes only. The structure exhibits idealized tetrahedral ( $T_d$ ) symmetry as indicated by the inscribed tetrahedron (yellow) that is introduced by the central templating anion  $[XO_4]^{n-}$ .

controlled geometrical changes, such as the different location of a given atom (positional isomerism) or a rotation of a fragment of the molecule (rotational isomerism). Baker and Figgis in 1970 postulated the existence of five isomers for the Keggin anion  $[XM_{12}O_{34}]^{3-}$  ( $X = As^V, P^V$ , etc.;  $M = Mo^{VI}, W^{VI}$ ) and six isomers for the Wells–Dawson anion  $[X_2M_{18}O_{62}]^{6-}$  ( $X = As^V, P^V$ , etc.;  $M = Mo^{VI}, W^{VI}$ ) [48]. Among the five isomers of the  $[PW_{12}O_{40}]^{3-}$ , the  $\alpha$  isomer is characterized by an assembly of four edge-sharing triads, W3 that share corners to each other in a tetrahedral fashion and has  $T_d$  symmetry. By successive  $60^\circ$  rotations of 1–4 triads (shaded octahedra), one gets the  $\beta$  ( $C_{3v}$ ),  $\gamma$  ( $C_{2v}$ ),  $\delta$  ( $C_{3v}$ ), and  $\epsilon$  ( $T_d$ ) isomers. The corresponding energy scale is commensurate with the experimental findings, showing that as the number of rotated triads increases, so does the energy of the metal oxide core, resulting in the order  $\alpha < \beta < \gamma < \delta < \epsilon$  [48]. As per isomer definition, their molecular formula remains the same, but their electrochemistry varies from isomer to isomer. A combination of experimental and theoretical data prove that the redox properties vary from isomer to isomer; however, fully oxidized Keggin anions prefer to adopt the  $\alpha$  arrangement, a result which has been further verified by theoretical evidence [49].

In the 1970, Baker and Figgis postulated six isomers for the Wells–Dawson anion:  $\alpha$ ,  $\beta$ ,  $\gamma$  and  $\alpha^*$ ,  $\beta^*$ ,  $\gamma^*$ . The  $\alpha$ -  $[X_2M_{18}O_{62}]^{q-}$  anion is built up from two  $A-\alpha-XM_9O_{34}$  half units joined by six common oxygen atoms, the structure belonging to  $D_{3h}$  point group. The  $\beta$  anion, see Figure 1.5, derives from  $\alpha$  isomer by a formal rotation by  $\pi/3$  of a polar (cap)  $M_3O_{13}$  group: the symmetry is lowered to  $C_{3v}$ . The formal rotation by  $\pi/3$  of the second polar  $M_3O_{13}$  group restores the symmetry plane and the point group  $D_{3h}$  for the  $\gamma$  isomer. In all these anions, the hexagonal belts of both  $XM_9$  moieties are symmetry related through the equatorial horizontal plane and their twelve tungsten atoms appear eclipsed along the direction of the  $C_3$ . If the two  $A-\alpha-XM_9O_{34}$  subunits are related through an inversion center, as postulated by Wells [34] in 1945 for  $[P_2W_{18}O_{62}]^{6-}$ , the resulting anion named  $\alpha^*$  would belong to the  $D_{3d}$  point group. Rotation of one or both polar (cap)  $M_3O_{13}$  groups of this  $\alpha^*$  anion would generate the two remaining isomers,  $\beta^*$  ( $C_{3v}$ ) and  $\gamma^*$  ( $D_{3d}$ ), respectively. In that case, the hexagonal belts of both  $XM_9$  moieties are symmetry related through the inversion center and their twelve tungsten atoms appear staggered along the direction of the  $C_3$  axis. Zhang *et al.* carried out density functional theory calculations to investigate  $\alpha$ ,  $\beta$ ,  $\gamma$ ,  $\alpha^*$ ,  $\beta^*$ , and  $\gamma^*$ - $[W_{18}O_{54}(PO_4)_2]^{6-}$  Wells–Dawson isomers, which exhibited stability in the order of  $\alpha > \beta > \gamma > \gamma^* > \beta^* > \alpha^*$ , reproduced the experimental observations ( $\alpha > \beta > \gamma$ ), and confirmed the hypothesis of Contant and Thouvenot ( $\gamma^* > \beta^* > \alpha^*$ ) [50].

Conventionally, redox-inactive anions, such as  $[SO_4]^{2-}$  and  $[PO_4]^{3-}$ , are often used as templating anions in the formation of many POM clusters. A strategy to create new functional POMs involves the encapsulation of redox-active templates instead. By utilizing sulfite, selenite, tellurite, and periodate anions as templates, several new types of redox-active heteropolyoxometalates have been isolated. The POM cluster  $[M_{18}O_{54}(SO_3)_2]^{3-}$  ( $M = W, Mo$ ), which contains two embedded redox-active sulfite templates, can be activated by a metallic surface

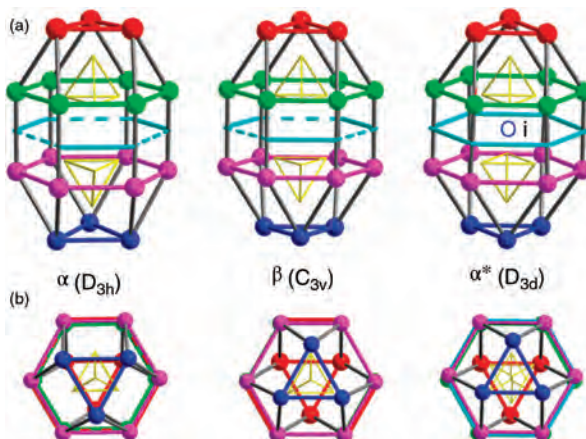


**Figure 1.5** (a) Rationalization of the 18 metal-centered  $\alpha$ ,  $\beta$ , and  $\alpha^*$  Wells–Dawson structures. (b) Views along the  $C_3$  axis. In the  $\alpha$  isomer, both CAP (red and blue) triads appear eclipsed along the  $C_3$ . On the contrary, the CAP triads appear staggered in the  $\beta$  and  $\alpha^*$  isomers. This is due to a  $\pi/3$  rotation of the blue CAP in the  $\alpha$  isomer that leads to the  $\beta$  anion. Another rotation of the red CAP in the  $\beta$  isomer derives in the  $\gamma$  isomer, not depicted here. The short–long alternation in the distances between the oxygens that interconnect both BELT units, depicted in turquoise, is maintained in the  $\alpha$ ,  $\beta$ , and  $\gamma$  isomers. If both CAP-BELT and A- $\alpha$ -XM<sub>9</sub>O<sub>34</sub> subunits are

related through an inversion center “*i*,” depicted in the figure, we obtain the  $\alpha^*$  isomer with a  $D_{3d}$  symmetry. In this case, the distance alternation between central oxygens (turquoise) disappears. The same happens with  $\beta^*$  and  $\gamma^*$ , since the oxygens are related through the improper axis  $S_6$ . Like  $\beta$  and  $\gamma$  isomers, a  $\pi/3$  rotation of the blue CAP in the  $\alpha^*$  isomer will lead to the  $\beta^*$  and the rotation of both CAP (blue and red) to  $\gamma^*$ . Note from part (b), vision along the  $C_3$  axis, the XO<sub>6</sub><sup>n-</sup> yellow octahedron appear eclipsed in  $\alpha$ ,  $\beta$ , consequently in  $\gamma$  isomers, whereas staggered in  $\alpha^*$  and subsequently in  $\beta^*$ ,  $\gamma$ .

and can reversibly interconvert between two electronic states [51]. Both templates can be replaced by a single template located in the center of the cluster to give a Dawson-like {W<sub>18</sub>X} POM [52]. The first member of this family to be discovered was actually an isopolyanion {W<sub>19</sub>} with a Dawson-type cage; the nineteenth tungsten is located at the center of the cluster instead of the two tetrahedral heteroatoms that are usually found inside conventional Dawson clusters [53]. Structural analysis of the cluster shows that the nineteenth tungsten could be replaced by other elements, such as Pt<sup>IV</sup>, Sb<sup>V</sup>, Te<sup>VI</sup>, or I<sup>VII</sup>. The POMs  $\beta^*$ -[H<sub>3</sub>W<sub>18</sub>O<sub>56</sub>(IO<sub>6</sub>)]<sup>6-</sup> embedded with high-valent iodine [54] and  $\gamma^*$ -[H<sub>3</sub>W<sub>18</sub>O<sub>56</sub>(TeO<sub>6</sub>)]<sup>7-</sup> that captures the tellurate anion [TeO<sub>6</sub>]<sup>6-</sup> were discovered thereafter (Figure 1.6) [55].

ESI-MS and DFT studies have been carried out to analyze the relative stability for a series of nonclassical WD anions. In contrast, for the nonclassical WD anions the obtained DFT stability order is  $\gamma^* > \beta^* > \alpha^* > \alpha > \beta > \gamma$  where the isomers  $\gamma^*$ ,  $\beta^*$ , and  $\alpha$  are the only anions of this type known to have been synthesized so far. The collision energy necessary to induce the total fragmentation of the {XW<sub>18</sub>} parent polyanion by ESI-MS was always found to be lower than the

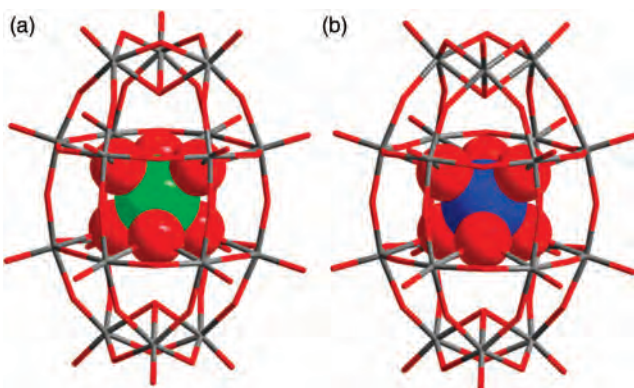


**Figure 1.6** Structures of the new Dawson-like  $\{W_{18}X\}$  POM type; the  $\{W_{18}\}$  cages are shown as sticks and the central  $\{XO_6\}$  group is represented as space filling model. (a)  $\gamma^*-[W_{18}O_{56}(XO_6)]^{10-}$   $X=W^{VI}$  and  $Te^{VI}$ . (b)  $\beta^*-[W_{18}O_{56}(VO_6)]^{9-}$  being the first example of  $\beta^*$  isomer.

homologous  $\{W_{19}\}$  species; binding energies predicted by DFT are in agreement with this general trend. We have been able to rationalize the isomerism in this new class of WD anions and explain their preference to adopt certain isomer structures [56].

We have also recently studied the transformation of the lacunary polyoxoanion  $[\beta_2\text{-SiW}_{11}\text{O}_{39}]^{8-}$  into  $[\gamma\text{-SiW}_{10}\text{O}_{36}]^{8-}$  using high-resolution electrospray mass spectrometry, density functional theory, and molecular dynamics. Using this approach we have demonstrated that the reaction mechanism proceeds through an unexpected  $\{\text{SiW}_9\}$  precursor that undertakes a direct  $\beta \rightarrow \gamma$  isomerization via a rotational transformation. The remarkably low-energy transition state of this transformation could be identified through theoretical calculations. Moreover, we explore the significant role of the countercations for the first time in such studies. This combination of experimental and the theoretical studies can now be used to understand the complex chemical transformations of oxoanions, leading to the design of reactivity by structural control [57].

Recently, Kondinsky *et al.* investigated computationally the  $\alpha$ -,  $\gamma$ -, and  $\beta$ -isomeric structures, relative stabilities, and the electronic and basicity properties of magnetic  $[V^{IV}_{14}E_8O_{50}]^{12-}$  (hereafter referred to as  $\{V_{14}E_8\}$ ) heteropolyoxovanadates (heteroPOVs) and their heavier chalcogenide-substituted  $[V^{IV}_{14}E_8O_{42}X_8]^{12-}$  ( $\{V_{14}E_8X_8\}$ ) derivatives for  $E=\text{Si}^{IV}$ ,  $\text{Ge}^{IV}$ , and  $\text{Sn}^{IV}$  and  $X=\text{S}$ ,  $\text{Se}$ , and  $\text{Te}$ . By using density functional theory (DFT) with scalar relativistic corrections in combination with the conductor-like screening model of solvation, they have accounted for the structure–property relations in heteroPOVs as well as to assist the synthesis and molecular deposition of these molecular vanadium-oxide spin clusters on surfaces. Their DFT calculations reveal stability trends  $\alpha > \gamma > \beta$  for polyoxoanions  $\{V_{14}E_8\}$  and  $\{V_{14}E_8X_8\}$ , based on relative energies and HOMO–LUMO energy gaps. Among  $\beta$  and  $\gamma$  isomers, the hitherto unknown

$\gamma\text{-}[V_{14}Sn_8O_{50}]^{12-}$  and  $\gamma\text{-}[V_{14}Sn_8O_{42}S_8]^{12-}$  seem to be the most viable targets for isolation. Furthermore, these Sn-substituted polyoxoanions are of high interest for electrochemical studies because of their capability to act as two-electron redox catalysts [58].

### 1.5 Building Blocks

One important factor that triggers the assembly of a set of building blocks into a particular POM species out of a vast number of possible candidates relates to the preferential stabilization of a specific building block library that can be used for the construction of larger aggregates. This point is brought into sharp focus when one realizes that, even though the POMs' structural features usually become the center of the researchers' attention, these POMs are still polyanions and cannot exist without the charge balancing cations that often define the network into which the anion is "complexed" and charge balance is achieved. In this way the cations themselves appear to be able to influence the existing equilibria in solution, provide stability of specific building blocks, and direct the assembly toward the formation and crystallization of a specific molecular candidate, see Figure 1.7.

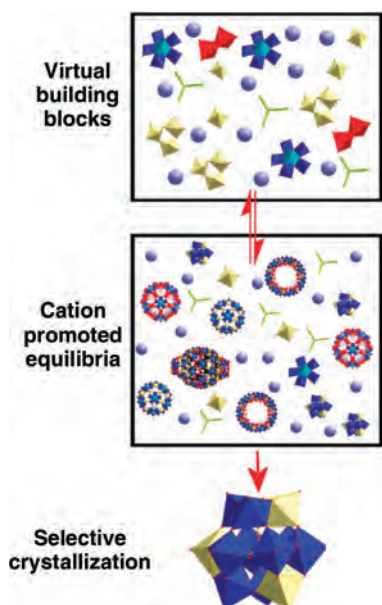
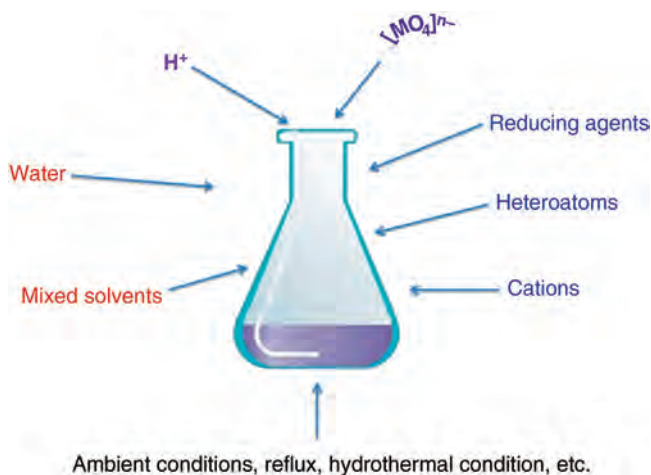


Figure 1.7 Schematic representation of the traditional "one-pot" synthesis of POM clusters leading to the formation of various structural archetypes in solution highlighting the role of counterions in selective stabilization, formation, and crystallization of a specific POM cluster.

Extensive research efforts over the last decades contributed towards our better understanding regarding the counterions' crucial effect on the self-assembly process that goes beyond simply maintaining the charge neutrality in the reaction mixture. Since the properties of the cations such as size, charge, coordination modes, symmetry, and solubility are found to modulate the reactivity as well as the stability of POM building blocks, these cations can clearly affect the nature of the product obtained from a POM synthesis [59]. Using a counterion directed self-assembly approach for the construction of novel POM species, there are two important points that need to be taken into consideration: (a) the generation of novel POM-based building block libraries and (b) promotion of their self-assembly in a controlled fashion to form novel architectures with potential useful functionality. The first option, in order to achieve these targets, is based on the use of bulky positively charged organic cations as counterions in the synthetic procedure [60–62]. The use of bulky cations such as hexamethylene tetramine (HMTA), triethanol amine (TEA), N,N-bis-(2-hydroxyethyl)-piperazine (BHEP), and morpholine prevents the rapid aggregation of POM-based synthons into clusters of stable and uniform spherical topology. Also, the use of cations in combination with transition metals as linker units are found to be capable of diversifying the population of the available constituents by stabilizing reactive secondary building units and directing their self-assembly into novel archetypes. The second option is based on the combined use of organic ligands and additional transition metals not only as counterions, but also as ligands, metal linkers, buffers, and even as redox reagents in some cases, in order to direct the self-assembly process toward a completely new direction [63,64]. Extensive use of the discussed approach gave researchers the opportunity to isolate a number of discrete iso- and heteropolyoxometalate clusters as well as many extended architectures using this simple but efficient concept.

## 1.6 Classic POM Synthesis

The incorporation of heteroatoms, heterometallic centers, lacunary building blocks, and cations and organic ligands have a profound effect on the self-assembly process and consequently the overall architecture. The architectural design principles used up until recently were based mainly on a fine balance of empirical observation and serendipity. In most cases, the utilized experimental procedures for producing POM-based clusters involves acidification of a solution of the chosen metallic salts, usually molybdates, tungstates, or vanadates [65] followed by a condensation process that involves the interaction of multiple building block libraries leading to the formation of a great variety of POM clusters. Traditionally, the synthesis of the POM cluster takes place in aqueous media and involves routine procedures requiring a small number or even just one step



**Figure 1.8** Parameters that are often adjusted in the synthesis/isolation of new POM clusters using the multiparameter one-pot method.

(“one-pot” synthetic approach) with many variables as already discussed (Figure 1.8) [66]. Recently, chemists are making efforts to re-evaluate their synthetic methodologies and adopt novel approaches that will lead to the designed synthesis of unique architectures (trapping of functional metallic cores, molecular nanoparticles, site specific activity) and potentially the emergence of novel properties (dynamic molecular organization, controlled oscillatory nano-devices, autocatalytic features) that are discussed further in detail.

## 1.7

### Novel Synthetic Approaches Using Flow Systems

Recently, we pioneered the use of a flow reactor system approach to both explore the mechanism and in the synthesis of complex polyoxometalate clusters. For example, by using the flow system we were able to generate a stationary kinetic state of the “intermediate” molybdenum-blue (MB) wheel, filled with a  $\{Mo_{36}\}$  guest to give a host–guest complex [67]. The MB host–guest complex has the form  $Na_{22}\{[Mo^{VI}_{36}O_{112}(H_2O)_{16}]\subset[Mo^{VI}_{130}Mo^V_{20}O_{442}(OH)_{10}(H_2O)_{61}]\cdot180H_2O\{Mo_{36}\}\subset\{Mo_{150}\}$ . Carrying out the reaction under controlled continuous flow conditions enabled selection for the generation of  $\{Mo_{36}\}\subset\{Mo_{150}\}$  as the major product, and allowed the reproducible isolation of this host–guest complex in good yield, as opposed to the traditional “one-pot” batch synthesis that typically leads to crystallization of the  $\{Mo_{154-x}\}$  species (Figure 1.9) [68]. Structural and spectroscopic studies identified the  $\{Mo_{36}\}\subset\{Mo_{150}\}$  compound as the intermediate in the synthesis of MB wheels. It is interesting to note that,

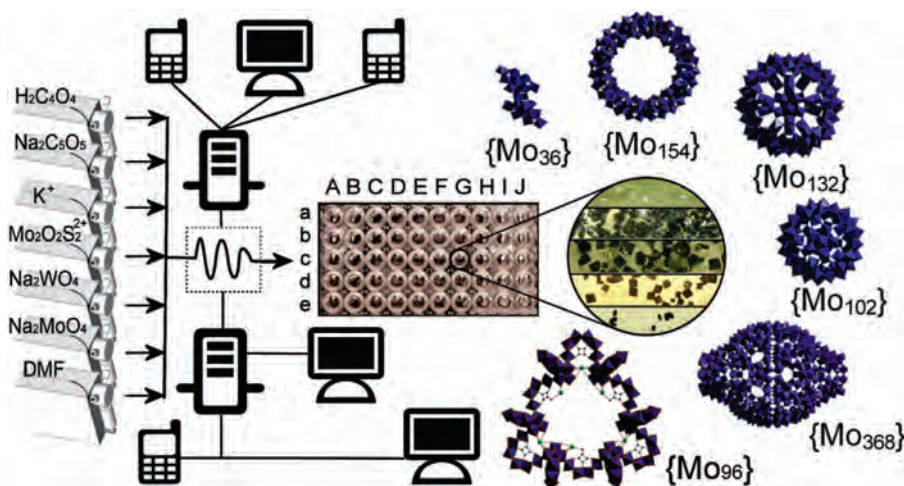


**Figure 1.9** Scheme of an automated system controlled by a PC that allows the discovery of new species.

compared to the archetypal 28 electron reduced “empty”  $\{Mo_{154}\}$  wheel, the  $\{Mo_{150}\}$  is only 20 electron reduced. This is of crucial importance since further reduction of the wheel results in the expulsion of the  $\{Mo_{36}\}$  guest indicating why this was not observed before reproducibly. Also, further experiments showed an increase in the yield and the formation rate of the  $\{Mo_{154-x}\}$  wheels by deliberate addition of preformed  $\{Mo_{36}\}$  to the reaction mixture. Dynamic light scattering (DLS) was also used to corroborate the mechanism of formation of the MB wheels through observation of the individual cluster species in solution. DLS measurement of the reaction mixtures, from which  $\{Mo_{36}\}$  and  $\{Mo_{150}\}$  crystallized, gave particle size distribution curves averaging 1.9 and 3.9 nm, respectively. The above approach allowed the use of size as a possible distinguishing feature of these key species in the reduced acidified molybdate solutions and direct observation of the molecular evolution of the available synthons to MB wheels [69].

Although the qualitative data obtained does not allow comprehensive kinetic studies at this stage, it brings us one step closer to understanding the formation of complicated systems like the MBs in solution. Using these techniques to follow the assembly of other self-assembled chemical systems in solution will open the door to further understanding and finally control of such complex self-assembly processes. The characterization of the “bottom-up” designed nanosized species in solution will also overcome the problems associated with product crystallization and isolation and will ultimately unveil the true potential of solution-processable nanosized metal oxides to be exploited in the manufacture of novel materials and molecular devices with engineered functionality.

### 1.8

#### Conclusions

One of the key aspects of the new developments at the frontiers of metal oxide cluster science is based on the finding that cluster structures are built on a hierarchy of template and templating subunits; however, this is not yet explored in detail. Also, it is just emerging that reaction networks based upon polyoxometalates can be increasingly treated as complex chemical systems containing inter-dependent networks of self-assembling, self-templating building blocks. Indeed, complex interacting “systems” defined using polyoxometalate building blocks may be used as the archetypal models to explore inorganic chemical networks.

The area of polyoxometalates is now entering into a new phase whereby it is possible to design and control both the structure and function of the systems. However, their dynamic nature with a seemingly endless structural diversity means that the assembly of functional nanomolecules and adaptive materials under nonequilibrium conditions will be developed. This approach will be used to access new building block libraries that will lead to the formation of novel nanomaterial structures and functions not accessible from near equilibrium processing techniques and will be focused on producing new materials, assemblies, and devices. Such processes may be driven using redox reactions, ion exchange, and metal unit substitution to drive, direct, and trap the self-assembly of molecular metal oxide-based building blocks, clusters, and materials in solution. By using such nonequilibrium-based processing, it will be a possible aim to engineer materials with unprecedented structures functionality and adaptive potential than possible with conventional, static, and near equilibrium self-assembly techniques. For example, in very recent work we have shown that it is possible to engineer cluster–guest compounds whereby a cluster-based oscillator is engineered, and the oscillation in the internal cluster template can be driven by the presence of a reducing amine in solution [70]. The fact that such dynamic behavior can be set up and observed in solution is exciting, and the coupling of such processes between the solution and solid-state has fantastic promise for the future design and discovery of polyoxometalate-based reaction systems and networks with emergent properties. We are confident that the structural explosion in the area of polyoxometalates will now lead to another explosion in functionality taking advantage of the transferable building blocks, and the ability to engineer nonequilibrium systems with unprecedented properties and emergent functionalities.

#### Acknowledgments

The authors would like to thank the University of Glasgow, WestCHEM, the EPSRC, Leverhulme Trust, the Royal Society/Wolfson Foundation, the Royal Society of Edinburgh, and Marie Curie actions for financial support as well as members of the Cronin laboratory, past and present.

## References

- 1 West, M.L. (ed.); Hesiod. (1966) *Theogony: Edited with Prolegomena and Commentary*. Clarendon Press, Oxford.
- 2 Russell, B. (1970) *A History of Western Philosophy*, Harcourt Brace Jovanovich, New York.
- 3 Descartes, R., Miller, V.R., and Miller, R.P. (1983) *Principles of Philosophy/René Descartes: Translated, with Explanatory Notes by Valentine Rodger Miller and Reese P. Miller*, Reidel, Dordrecht, London.
- 4 Jones, R. (2008) *Soft Machines – Nanotechnology and Life*, Oxford University Press, Oxford.
- 5 Whitesides, G.M. and Grzybowski, B. (2002) *Science*, **295**, 2418–2421.
- 6 Altamura, L. (2016) Self-assembly: Latest research and news – Nature. Available at <http://www.nature.com/subjects/self-assembly> (accessed Nov. 2, 2016).
- 7 Bensaude-Vincent, B. (2006) Self-assembly, Self-organization: a philosophical perspective on converging technologies, paper prepared for France/Stanford Meeting Avignon, December 2006. Available at <http://stanford.edu/dept/france-stanford/Conferences/Ethics/BensaudeVincent.pdf> (accessed Nov. 2, 2016).
- 8 Prigogine, I., Stengers, I., and Toffler, A. (1984) *Order out of Chaos*, Bantam Books, New York.
- 9 Petrov, V., Gaspar, V., Maesere, J., and Showalter, K. (1993) *Nature*, **361**, 240–243.
- 10 England, J. (2015) *Nat. Nanotech.*, **10**, 919–923.
- 11 Macklem, P.T. (2008) *J. Appl. Physiol.*, **104**, 1844–1846.
- 12 Ozin, G.A., Hou, K., Lotsch, B.V., Cademartiri, L., Puzzo, D.P., Scotognella, F., Ghadimi, A., and Thomson, J. (2009) *Mater. Today*, **12**, 12–23.
- 13 Desiraju, G.R. (1989) *Crystal Engineering: The Design of Organic Solids*, Elsevier, New York.
- 14 Evans, D.F. and Wennerstrom, H. (1999) *The Colloidal Domain: Where Physics, Chemistry, Biology, and Technology Meet*, John Wiley & Sons, New York.
- 15 Jones, M.N. and Chapman, D. (1995) *Micelles, Monolayers, and Biomembranes*, Wiley–Liss, New York.
- 16 Jakubith, S., Rotermund, H.H., Engel, W., von Oertzen, A., and Ertl, G. (1990) *Phys. Rev. Lett.*, **65**, 3013–3016.
- 17 Hess, B. (2000) *Naturwissenschaften*, **87**, 199–211.
- 18 Whitesides, G.M. and Boncheva, M. (2002) *PNAS*, **99**, 4769–4774.
- 19 Cademartiri, L. and Ozin, G.A. (2009) *Concepts of Nanochemistry*, Wiley-VCH Verlag GmbH, Weinheim.
- 20 Drexler, E. (1986) *Engines of Creation: The Coming Era of Nanotechnology*, Anchor Books, New York.
- 21 Pope, M.T. and Müller, A. (1991) *Angew. Chem., Int. Ed. Engl.*, **30**, 34–48.
- 22 Berzelius, J. (1826) *Poggendorff's Ann. Phys.*, **6**, 369–380.
- 23 Keggan, J.F. (1934) *Proc. R. Soc. A.*, **144**, 75.
- 24 Hill, C.L. (1998) *Chem. Rev.*, **98**, 1–2.
- 25 Pope, M.T. and Müller, A. (1994) *Polyoxometalates: From Platonic Solids to Anti-Retroviral Activity*, Kluwer Academic Publishers, Dordrecht.
- 26 (a) Proust, A., Matt, B., Villanneau, R., Guillemot, G., Gouzerh, P., and Izzet, G. (2012) *Chem. Soc. Rev.*, **41**, 7605–7622; (b) Yu-Fei, S. and Ryo, T., (2012) *Chem. Soc. Rev.*, **41**, 7384–7402; (c) Miras, H.N., Yan, J., Long, D.-L., and Cronin, L., (2012) *Chem. Soc. Rev.*, **41**, 7403–7430; (d) Long, D.-L., Burkholder, E. and Cronin, L., (2007) *Chem. Soc. Rev.*, **36**, 105–121.
- 27 Pope, M.T. (1983) *Heteropoly and Isopoly Oxometalates*, Springer, New York.
- 28 Müller, A. and Roy, S. (2004) *The Chemistry of Nanomaterials: Synthesis, Properties and Applications*, Wiley-VCH Verlag GmbH, Weinheim.
- 29 (a) Miras, H.N., Wilson, E.F. and Cronin, L. (2009) *Chem. Commun.*, 1297–1311; (b) Wilson, E.F., Miras, H.N., Rosnes, M.H., and Cronin, L., (2011) *Angew. Chem., Int. Ed.*, **50**, 3720–3724; (c) Sartorel, A., Carraro, M., Scorrano, G., De Zorzi, R., Geremia, S., McDaniel, N.D., Bernhard, S., and Bonchio, M., (2008) *J. Am. Chem. Soc.*, **130**, 5006–5007; (d) Geletii, Y.V., Botar, B., Köegerler, P.,

- Hillesheim, D.A., Musaev, D.G., and Hill, C.L., (2008) *Angew. Chem., Int. Ed.*, **47**, 3896–3899; (e) Sartorel, A., Miró, P., Salvadori, E., Romain, S., Carraro, M., Scorrano, G., Di Valentin, M., Llobet, A., Bo, C., and Bonchio, M., (2009) *J. Am. Chem. Soc.*, **131**, 16051–16053; (f) Zheng, Q., Vilà-Nadal, L., Busche, C., Mathieson, J.S., Long, D.-L., and Cronin, L. (2015) *Angew. Chem., Int. Ed.*, **54**, 7895–7899.
- 30** (a) Kamata, K., Yonehara, K., Sumida, Y., Yamaguchi, K., Hikichi, S., and Mizuno, N. (2003) *Science*, **300**, 964–966; (b) Kim, W.B., Voitl, T., Rodriguez-Rivera, G.J., and Dumesic, J.A. (2004) *Science*, **305**, 1280–1283; (c) Nyman, M., Bonhomme, F., Alam, T.M., Rodriguez, M.A., Cherry, B.R., Krumhansl, J.L., Nenoff, T.M., and Sattler, A.M. (2002) *Science*, **297**, 996–998; (d) Miras, H.N., Cooper, G.J.T., Long, D.-L., Bogge, H., Müller, A., Streb, C., and Cronin, L. (2010) *Science*, **327**, 72–74; (e) Rausch, B., Symes, M.D., Chisholm, G., and Cronin, L. *Science*, (2014) **345**, 1326–1330; (f) Douglas, T. and Young, M. (1998) *Nature*, **393**, 152–155; (g) Müller, A., Shah, S.Q.N., Bogge, H., and Schmidtmann, M. (1999) *Nature*, **397**, 48–50; (h) Neumann, R. and Dahan, M. (1997) *Nature*, **388**, 353–355; (i) Weinstock, I.A., Barbuzzi, E.M.G., Wemple, M.W., Cowan, J.J., Reiner, R.S., Sonnen, D.M., Heintz, R.A., Bond, J.S., and Hill, C.L. (2001) *Nature*, **414**, 191–195; (j) Busche, C., Vilà-Nadal, L., Yan, J., Miras, H.N., Long, D.-L., Georgiev, V.P., Asenov, A., Pedersen, R.H., Gadegaard, N., Mirza, M.M., Paul, D.J., Poblet, J.M., and Cronin, L. (2014) *Nature*, **515**, 545–549; (k) Shiddiq, M., Komijani, D., Duan, Y., Gaita-Ariño, A., Coronado, E., and Hill, S. (2016) *Nature*, **531**, 348–351; (l) Coronado, E., Galán-Mascarós, J.R., Gómez-García, C.J., and Laukhin, V. (2000) *Nature*, **408** 447–449.
- 31** Müller, A., Reuter, H., and Dillingen, S. (1995) *Angew. Chem., Int. Ed. Engl.*, **34**, 2328–2361.
- 32** Müller, A., Beckmann, E., Böggel, H., Schmidtmann, M., and Dress, A. (2002) *Angew. Chem., Int. Ed.*, **41**, 1162–1167.
- 33** Lindqvist, I. (1952) *Acta Crystallogr.*, **5**, 667.
- 34** (a) Keggin, F.J. (1933) *Nature*, **131**, 908; (b) Keggin, F.J. (1934) *Proc. R. Soc. Lond., A* **144**, 75; (c) Wells, A.F. (1945) *Structural Inorganic Chemistry*, Oxford University, Oxford; (d) Dawson, B. (1953) *Acta Crystallogr.*, **6**, 113.
- 35** (a) Preyssler, C. (1970) *Bull. Soc. Chim. Fr.*, 30; (b) Alizadeh, M.H., Harmalker, S.P., Jeannin, Y., Martin-Frère, J., and Pope, M.T. (1985) *J. Am. Chem. Soc.*, **107**, 2662–2669.
- 36** (a) Müller, A., Böggel, H. and Diemann, E. (2003) *Inorg. Chem. Commun.*, **6**, 52–53; (b) Corrigendum: Müller, A., Böggel, H. and Diemann, E., (2003) *Inorg. Chem. Commun.*, **6**, 329; (c) Garcia-Ratés, M., Miró, P., Poblet, J.M., Bo, C., and Avalo, J.B., (2011) *J. Phys. Chem. B*, **115**, 5980–5992.
- 37** (a) Long, D.-L., Tsunashima, R., and Cronin, L. (2010) *Angew. Chem., Int. Ed.*, **49**, 1736–1758; (b) Long, D.-L. and Cronin, L. (2006) *Chem. Eur. J.*, **12**, 3698–3706.
- 38** (a) Cronin, L. (2004) *High Nuclearity Clusters: Iso and Heteropolyoxoanions and Relatives: Comprehensive Coordination Chemistry II*, vol. 7 (eds J.A. McCleverty and T.J. Meyer), Elsevier, Amsterdam, pp. 1–56; (b) Long, D.-L., Kögerler, P., Farrugia, L.J., and Cronin, L., (2003) *Angew. Chem., Int. Ed.*, **42**, 4180–4183; (c) Miras, H.N., Yan, J., Long, D.-L., and Cronin, L., (2008) *Angew. Chem., Int. Ed.*, **47**, 8420–8423.
- 39** Long, D.-L., Kögerler, P., and Cronin, L. (2004) *Angew. Chem., Int. Ed.*, **43**, 1817–1820.
- 40** Müller, A., Krickemeyer, E., Meyer, J., Böggel, H., Peters, F., Plass, W., Diemann, E., Nonnenbruch, F., Randerath, M., and Menke, C. (1995) *Angew. Chem., Int. Ed. Engl.*, **34**, 2122–2124.
- 41** Müller, A., Krickemeyer, E., Böggel, H., Schmidtmann, M., and Peters, F. (1998) *Angew. Chem., Int. Ed.*, **37**, 3359–3363.
- 42** (a) Symes, M.D., Kitson, P.J., Yan, J., Richmond, C.J., Cooper, G.J.T., Bowman, R.W., Vilbrandt, T., and Cronin, L. (2012) *Nat. Chem.*, **4**, 349–354; (b) Kitson, P.J., Marshall, R.J., Long, D.-L., Forgan, R.S., and Cronin, L., (2014) *Angew. Chem., Int. Ed.*, **53**, 12723–12728; (c) de la Oliva, A.R.,

- Sans, V., Miras, H.N., Yan, J., Zang, H., Richmond, C.J., Long, D.-L., and Cronin, L., (2012) *Angew. Chem., Int. Ed.* **51**, 12759–12762.
- 43** (a) Vilà-Nadal, L., Rodríguez-Forteá, A., Yan, L.K., Wilson, E.F., Cronin, L., and Poblet, J.M. (2009) *Angew. Chem., Int. Ed.*, **48**, 5452–5456; (b) Vilà-Nadal, L., Rodríguez-Forteá, A., and Poblet, J.M. (2009) *Eur. J. Inorg. Chem.*, **2009**, 5125–5133; (c) Vilà-Nadal, L., Wilson, E.F., Miras, H.N., Rodríguez-Forteá, A., Cronin, L., and Poblet, J.M. (2011) *Inorg. Chem.*, **50**, 7811–7819; (d) Rodríguez-Forteá, A., Vilà-Nadal, L., and Poblet, J.M. (2008) *Inorg. Chem.*, **50**, 7745–7750.
- 44** Lang, Z.-L., Guan, W., Yan, L.-K., Wen, S.-Z., Su, Z.-M., and Haob, L.-Z. (2012) *Dalton Trans.*, **41**, 11361–11368.
- 45** Vilà-Nadal, L., Mitchell, S.G., Rodríguez-Forteá, A., Miras, H.N., Cronin, L., and Poblet, J.M. (2011) *Phys. Chem. Chem. Phys.*, **13**, 20136–20145.
- 46** Lang, Z.-L., Guan, W., Wub, Z.-J., Yan, L.-K., and Su, Z.-M. (2012) *Comput. Theor. Chem.*, **999**, 66–73.
- 47** (a) Strickland, J.D.H. (1952) *J. Am. Chem. Soc.*, **74**, 862–867; (b) Strickland, J.D.H. (1952) *J. Am. Chem. Soc.*, **74**, 872–876; (c) Strickland, J.D.H. (1952) *J. Am. Chem. Soc.*, **74**, 868–871.
- 48** (a) Baker, L.C.W. and Figgis, J.S. (1970) *J. Am. Chem. Soc.*, **92**, 3794–3797; (b) Hervé, G. and Tézé, A. (1977) *Inorg. Chem.*, **16**, 2115–2117.
- 49** López, X. and Poblet, J.M. (2004) *Inorg. Chem.*, **43**, 6863–6865.
- 50** Zhang, F.-Q., Guan, W., Yan, L.-K., Zhang, Y.-T., Xu, M.-T., Hayfron-Benjamin, E., and Su, Z.-M. (2011) *Inorg. Chem.*, **50**, 4967–4977.
- 51** (a) Fleming, C., Long, D.-L., McMillan, N., Johnston, J., Bovet, N., Dhanak, V., Gadegaard, N., Kögerler, P., Cronin, L., and Kadodwala, M. (2008) *Nat. Nanotechnol.*, **3**, 229–233; (b) Fay, N., Bond, A.M., Baffert, C., Boas, J.F., Pilbrow, J.R., Long, D.-L., and Cronin, L. (2007) *Inorg. Chem.*, **46**, 3502–3510.
- 52** Long, D.-L., Song, Y.F., Wilson, E.F., Kögerler, P., Guo, S.X., Bond, A.M., Hargreaves, J.S.J., and Cronin, L. (2008) *Angew. Chem., Int. Ed.*, **47**, 4384–4387.
- 53** Long, D.-L., Kögerler, P., Parenty, A.D.C., Fielden, J., and Cronin, L. (2006) *Angew. Chem., Int. Ed.*, **45**, 4796–4798.
- 54** Vilà-Nadal, L., Peuntinger, K., Busche, C., Yan, J., Lüders, D., Long, D.-L., Poblet, J.M., Guldi, D.M., and Cronin, L. (2013) *Angew. Chem., Int. Ed.*, **52**, 9695–9699.
- 55** Yan, J., Long, D.-L., Wilson, E.F., and Cronin, L. (2009) *Angew. Chem., Int. Ed.*, **48**, 4376–4380.
- 56** Vilà-Nadal, L., Mitchell, S.G., Long, D.-L., Rodríguez-Forteá, A., López, X., Poblet, J.M., and Cronin, L. (2012) *Dalton Trans.*, **41**, 2264–2271.
- 57** Cameron, J.M., Vilà-Nadal, L., Winter, R.S., Iijima, F., Murillo, J.C., Rodríguez-Forteá, A., Oshio, H., Poblet, J.M., and Cronin, L. (2016) *J. Am. Chem. Soc.*, **138**, 8765–8773.
- 58** Kondinski, A., Heine, T., and Monakhov, K.Y. (2016) *Inorg. Chem.*, **55**, 3777–3788.
- 59** (a) Contant, R. (1990) *Inorganic Syntheses*, vol. 27, John Wiley & Sons, New York, 109; (b) Contant, R. and Ciabrini, J.P., (1977) *J. Chem. Res. Miniprint*, 2601–2617; (c) Contant, R. and Ciabrini, J.P., (1977) *J. Chem. Res. Synop.*, 222; (d) Knoth, W.H. and Harlow, R.L., (1981) *J. Am. Chem. Soc.*, **103**, 1865–1867; (e) Cann, J., Tézé, A., Thouvenot, R., and Hervé, G., (1986) *Inorg. Chem.*, **25**, 2114–2119; (f) Kirby, J.F. and Baker, L.C.W., (1998) *Inorg. Chem.*, **37**, 5537–5543.
- 60** Yan, J., Long, D.-L., Miras, H.N., and Cronin, L. (2010) *Inorg. Chem.*, **49**, 1819–1825.
- 61** Miras, H.N., Stone, D.J., McInnes, E.J.L., Raptis, R.G., Baran, P., Chilas, G.I., Sigalas, M.P., Kabanos, T.A., and Cronin, L. (2008) *Chem. Commun.*, 4703–4705.
- 62** Miras, H.N., Ochoa, M.N.C., Long, D.-L., and Cronin, L. (2010) *Chem. Commun.*, **46**, 8148–8150.
- 63** Sartzi, C., Miras, H.N., Vilà-Nadal, L., Long, D.-L., and Cronin, L. (2015) *Angew. Chem., Int. Ed.*, **54**, 15708–15712.
- 64** Miras, H.N., Sorus, M., Hawkett, J., Sells, D.O., McInnes, E.J.L., and Cronin, L. (2012) *J. Am. Chem. Soc.*, **134**, 6980–6983.
- 65** Ritchie, C., Streb, C., Thiel, J., Mitchell, S.G., Miras, H.N., Long, D.-L., Peacock, R.D., McGlone, T., and Cronin, L. (2008) *Angew. Chem., Int. Ed.*, **47**, 6881–6884.

- 66** (a) Hill, C.L. and Prosser-McCartha, C.M. (1995) *Coord. Chem. Rev.*, **143**, 407–455; (b) Dolbecq, A., Dumas, E., Mayer, C.R., and Mialane, P., (2010) *Chem. Rev.*, **110**, 6009–6048.
- 67** Miras, H.N., Cooper, G.J.T., Long, D.-L., Bogge, H., Müller, A., Streb, C., and Cronin, L. (2010) *Science*, **327**, 72–74.
- 68** Miras, H.N., Richmond, C.J., Long, D.-L., and Cronin, L. (2012) *J. Am. Chem. Soc.*, **134**, 3816–3824.
- 69** Ibrahim, M., Mal, S.S., Bassil, B.S., Banerjee, A., and Kortz, U. (2011) *Inorg. Chem.*, **50**, 956–960.
- 70** Takashima, Y., Miras, H.N., Glatzel, S., and Cronin, L. (2016) *Chem. Commun.*, **52**, 7794–7797.